Superorbital expansion tube operation: Estimates of flow conditions via numerical simulation

P. A. Jacobs* T. B. Silvester† R. G. Morgan‡ M. P. Scott§
R. J. Gollan¶ and T. J. McIntyre‖
Center for Hypersonics, The University of Queensland, Brisbane 4072, Australia

Two new operating conditions of the X3 superorbital expansion tube are studied experimentally and numerically. A two-stage numerical simulation is used to model the flow processes within the whole facility, from the compressed driver gas, through the initial shock-processing of the test gas and then through the unsteady expansion process to the final test flow state. Experimental measurements provide static pressure histories at particular points along the shock and acceleration tubes while the numerical simulations provide complementary information on gas density, temperature and composition. Operating condition properties such as shock speed are both observed in the experiment and produced as a result of the simulation are used to check the reliability of the numerical simulations.

I. Introduction

Free-piston driven expansion tubes[1,2] are of interest because they can be used to provide aerothermodynamic data for flow speeds well in excess of 10 km/s and can use a range of test gases to simulate spacecraft entry into the atmospheres of Mars, Neptune and Titan, for example. Also, they have been recommended for use in scramjet testing because of the possibility of generating very large dynamic pressures.[3]

Experimental studies using expansion tube facilities, such as the ballute study by McIntyre,[4] typically examine the aerothermodynamic environment of a model spacecraft. Although these studies are primarily to obtain experimentally measured pressure and heat transfer data, numerical simulations play a role in obtaining that data. Because few of the properties of the test flow can be measured directly, numerical simulations, starting with operating parameters that can be measured, are used to estimate the full set of test flow properties. Past investigations of free-piston expansion tubes by Neely[5] and Palmer[6] have used a relatively simple one-dimensional analysis of the expansion tube process based on equilibrium chemistry. In practice, the flow processes are confused by many interacting phenomena such as finite-rate chemical kinetics, ionization, viscous effects (such as the developing boundary layer on the tube wall), and other unsteady flow processes (possibly caused by a non-ideal driver) which are not included in the simplified models.

A more recent investigation[7] indicated that reasonably good estimates of the test flow conditions in a small expansion tube facility (X2) could be obtained by simulating just the downstream-end of the shock tube and all of the acceleration tube. Fixed flow conditions were applied at the junction between the shock tube and the acceleration tube. The present study extends that work by considering the newer and much larger X3 facility, which is presently capable of producing steady test flows up to 8.5 km/s for periods of approximately 400 μs. Special consideration is given to modelling the non-ideal operating conditions in the shock tube and to undertaking axisymmetric simulations of the acceleration tube with finite-rate chemical models, for nitrogen and air as the test gases.

*Lecturer, Department of Mechanical Engineering, The University of Queensland.
†Graduate student, Department of Mechanical Engineering, The University of Queensland.
‡Professor, Department of Mechanical Engineering, The University of Queensland.
§Graduate student, Department of Mechanical Engineering, The University of Queensland.
¶Graduate student, Department of Mechanical Engineering, The University of Queensland.
‖Research Fellow, Department of Physics, The University of Queensland.

II. The X3 facility: description and operation

The X3 facility has a total length of 65 m and an exit diameter of 0.183 m with a usable test core flow of approximately 0.14 m. A schematic of X3 is shown in Fig. 1; comprised of a combined compression tube length of 25 m with bore diameters of 0.5 m and 0.2 m, a shock tube length of 12.5 m and bore diameter of 0.180 m and an acceleration tube length of 24 m and diameter of 0.183 m.

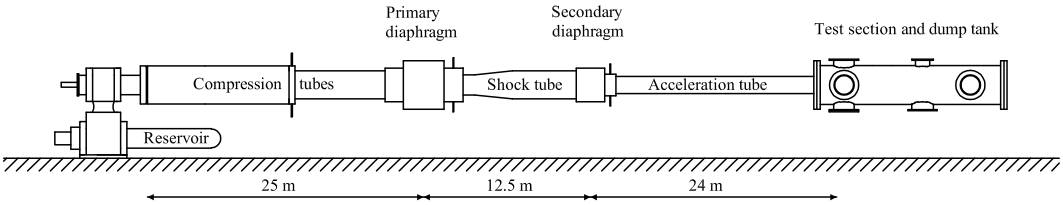

Figure 1. Schematic of the X3 Superorbital Expansion Tube (not to scale).

An idealized $x - t$ diagram of the flow processes discussed above associated with the operation of the X3 expansion tube is shown in Fig. 2. The operation of X3 relies on a two-stage free-piston driver, with a combined piston mass of 450 kg, to generate a high temperature compressed driver gas. The compression process transfers the piston's kinetic energy to the driver gas which stores the energy temporarily. Time zero in the figure corresponds to the end of the piston stroke and the rupture of the primary diaphragm (that was caused by increase in pressure of the driver gas required to bring the piston to rest). For the present operating conditions, the 1.6 mm mild steel primary diaphragm ruptures at a pressure of approximately 11 MPa.

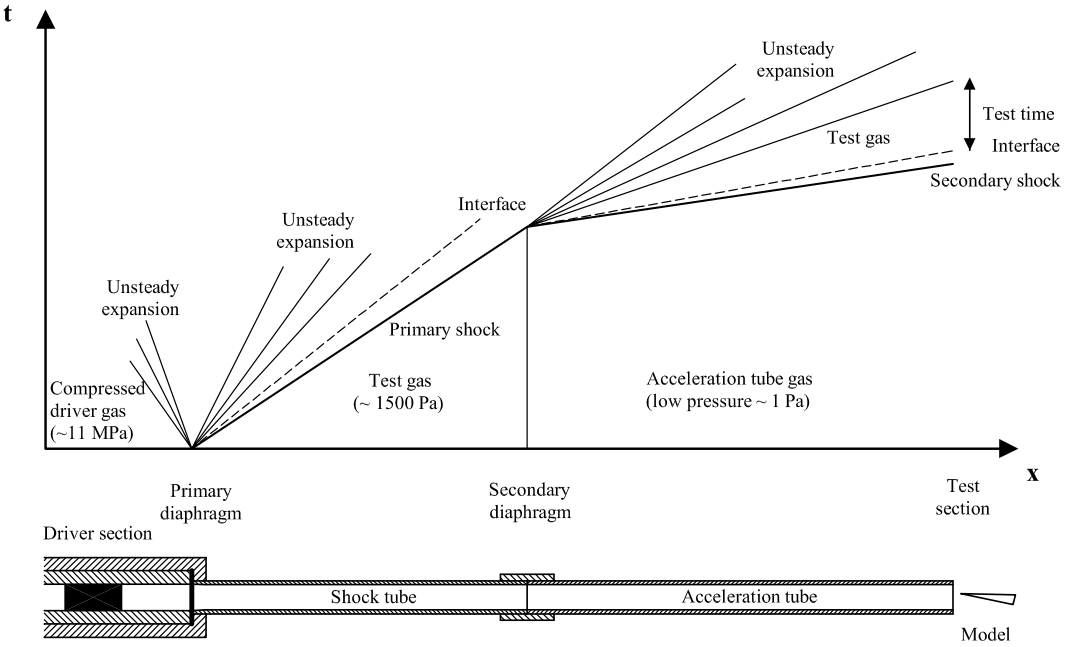

Figure 2. Idealized x-t diagram of the operation of the X3 facility.

Rupture of the primary diaphragm creates a shock wave that travels along the shock tube compressing and accelerating the test gas. Since the test gas is retained in the shock tube only by a *light* secondary diaphragm, the rupture of the secondary diaphragm (upon shock arrival) allows the compressed test gas to expand into the acceleration tube, pushing a low-pressure *acceleration* gas before it. This second stage of processing of the test gas through a strong unsteady expansion fan (centred at the secondary diaphragm

station) accelerates the test gas into the test section at speeds in excess of 8 km/s. The presence of the acceleration gas regulates the amount of expansion that the test gas experiences.

The operation of an expansion tube differs slightly from the more conventional reflected-shock tube in that energy is added to the flow in part by the shock wave with the remainder added via an unsteady expansion centred at both diaphragm stations. In this way, total enthalpy and total pressure are added to the flow without the levels of freestream dissociation that would occur if all the energy were added by a shock wave, as is the case with shock tunnels. The operation of expansion tubes allow higher energy flows to be realized at the expense of reduced test times. Further details of the principles and operation are reported by Neely & Morgan[8] and Morgan.[9]

For test conditions used in this study, the primary and secondary shock speeds were nominally 4150 m/s and 8300 m/s respectively. As illustrated in the $x - t$ diagram, the nominal test time commences following the passage of the starting shock (secondary shock) and the interface separating the acceleration and test gas and is terminated by the arrival of upstream expansion waves. Based on a Mirels analysis,[10] the time between of the shock and interface is 2 μs.

For the current investigation, the nominal filling conditions are listed in Table 1.

Table 1. Filling pressures for the nominal X3 flow conditions.

Condition	Reservoir (MPa Air)	Compression Tube Gas Composition (%He/%Ar)	Compression Tube (kPa)	Shock Tube (Pa Test Gas)	Acceleration Tube (Pa Air)
Air	1.3	100/0	17.2	1500 Air	0.9
N_2	1.3	100/0	17.2	1500 N_2	0.9

III. Estimation of test-flow conditions via simulation

The flow conditions at the end of the acceleration tube are estimated from a mix of measurements and calculations. Parameters that can be directly measured are the initial fill pressures and temperatures, the shock speeds and the static pressures at a number of locations in both the shock tube and the acceleration tube.

A. One-dimensional modelling of the shock tube

Ideally, the flow conditions in the shock tube could be estimated by starting with the post-shock static pressure p_2 and the initial fill temperature T_1 in the shock tube and combining this information with the incident shock speed as measured by time-of-flight toward the end of the shock tube. A one-dimensional flow model, assuming equilibrium chemistry, could be applied and the remaining pre- and post-shock conditions computed. However, the X3 facility is only recently commissioned and its operating conditions are still being optimized. Presently, it is operated with a driver that results in noticeable attenuation of the primary shock.

To accommodate this attenuation, the flow data in the shock tube are estimated from a one-dimensional simulation of the downstream part of the driver and whole of the shock tube using the L1d code.[11] The distance between the piston and main diaphragm and the driver temperature, at main-diaphragm rupture, have been adjusted to provide a good approximation to the two pressure histories measured in the shock tube. This adjustment considers, shock speed, peak pressures and pulse duration. Figure 3 shows the resulting comparison between measured and L1d simulation data for one of the shots with nitrogen as the test gas. There are some continuing difficulties with obtaining clean experimental data but we seem to be modelling the essential features adequately. The transient inflow properties are obtained from the downstream location (corresponding to the trace with its peak at 3 milliseconds).

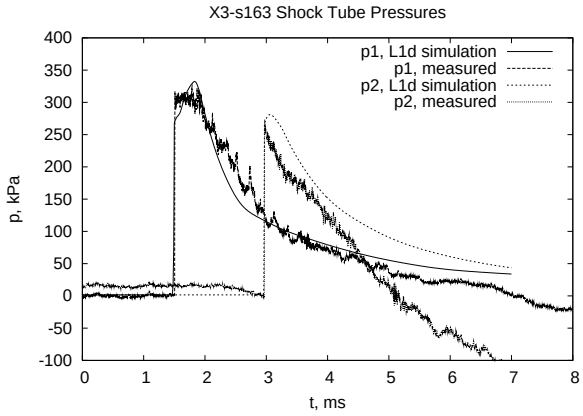

Figure 3. Shock tube pressure histories for X3 shot 163.

B. Axisymmetric modelling of the acceleration tube

The post-shock conditions in the shock tube are then used as an inflow boundary condition for an axisymmetric viscous flow simulation of the unsteady expansion process in the acceleration tube. This simulation is done with the MB_CNS code [12,13] and either an equilibrium-chemistry lookup table generated with the CEA code [14] or a finite-rate single-temperature thermochemical model of the test gas.[15] See the Appendix for details of the reaction model used for air.

The geometry of the simulated sections of the X3 facility are shown schematically in Fig. 4. The downstream-end of the shock tube is labelled as block 0 and the acceleration tube is divided into a further N blocks.

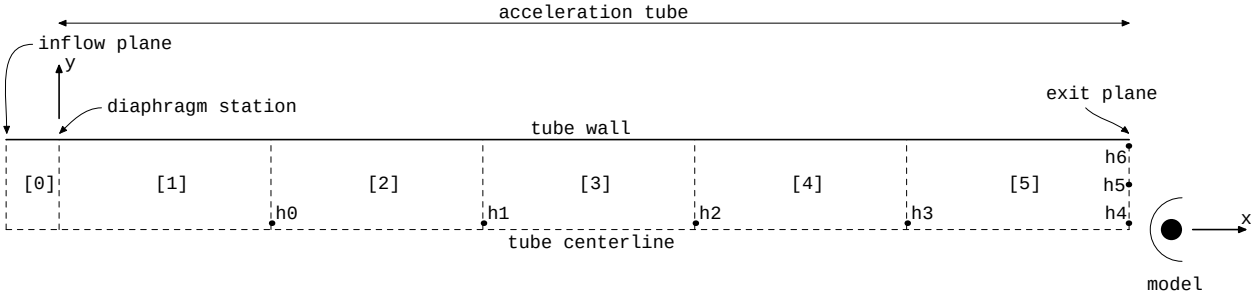

Figure 4. Schematic diagram of the simulation domain for the X2 facility.

During the axisymmetric simulation, test gas with post-shock conditions (as computed by the one-dimensional simulation of the shock tube) is placed in block 0 and at the inflow boundary. In the real facility, the light secondary diaphragm has a significant mass when compared with the total mass of gas initially in the acceleration tube. The impact of the shocked test gas on the secondary diaphragm leads to a temporary reverse shock that may affect the processing of the test gas that is eventually expanded to final test-flow conditions. Although, no reverse shock wave was included in the current simulations, its influence can be significant[16,17] and some form of reverse shock model should be included in future work.

The simulation proceeds by integrating the finite-volume form of the compressible Navier-Stokes equations with an explicit time-stepping scheme. MB_CNS is a shock capturing type code so the incident shock, contact surface, unsteady expansion and tube-wall boundary layer all develop within the flow field. The division of the flow domain into several blocks allows the simulation of each block to be calculated in parallel with an exchange of interblock boundary data at each time step. These calculations are expensive and, as noted by Wilson,[17] the grid reolution that we can achieve is limited by the available computational

resources. The highest resolution calculation of the flow in the acceleration tube for the air condition used approximately 11,500 CPU-hours on our cluster computer. This particular calculation had 121320 finite-volume cells distributed over 50 Opteron processors.

Much like the experimental measurements, the principal data used to estimate the freestream conditions are in the form of flow property histories recorded at points labelled h0 through h6 in Fig. 4. Shock speed is estimated from the time of flight between the sample points as indicated by static pressure histories. The other flow conditions are interpolated from the histories at the sample points close to the end of the acceleration tube. Estimates of the freestream conditions were obtained by averaging the simulated results over a chosen time interval where the simulated and experimental pressure histories matched. Time histories of the simulated and measured static pressure close to the end of the acceleration tube showing the averaging interval is shown in Fig. 5.

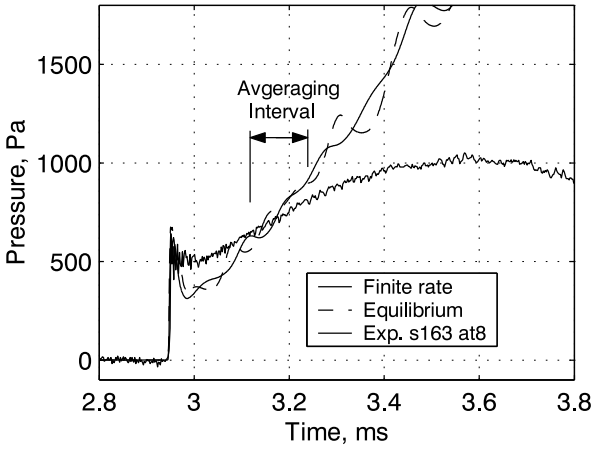

Figure 5. Experimental and CFD pressure histories at acceleration tube exit, showing time interval where numerical estimates of the flow conditions were averaged (shot s163).

The nominal freestream conditions for the nitrogen tests are listed in Table 2 for equilibrium and finite-rate thermochemistry. Similarly the nominal freestream conditions for the air test are listed in Table 3. Experimental measurements from the limited diagnostics are listed for comparison. As to be expected, the equilibrium simulation predicts a higher temperature than the finite-rate simulation. However, some amount of freestream dissociation and thus a lower temperature is expected due the reflected shock at the secondary diaphragm.[16] Furthermore, the estimated Pitot pressure, static pressure and shock speed differ slightly from the measured values, to within experimental uncertainty being, -6%, -4% and +3% respectively. In the experiment, Mach number of the test gas is deduced from the shock angle on the the leading edge of a duct placed just downstream of the exit of the acceleration tube. Holographic interferometry was used to visualize the test-section flow.

Tables 2 and 3 also include JUMP predictions of the test conditions. JUMP utilizes a simplified one-dimensional inviscid model of the expansion tube flow process and is the main technique used in past studies to estimate the test conditions. JUMP incorporates a *freezing* velocity in which the equilibrium state of the gas is frozen at a user-specified velocity through the unsteady expansion. This velocity is iterated until the measured Pitot and static pressures match the predictions. Simulation of the flow further downstream into the test section[18] indicates that the accuracy of these JUMP predictions is questionable because there is an immediate and strong change in chemical composition of the gas. In the case of the X3 facility, it is expected that any chemical reactions occurring in the test gas should be minimal by the time the gas slug reaches the test section. Numerical estimates of the three-dimensional flow within a rectangular duct based on the finite-rate test conditions presented here are in good agreement with the experimental skin-friction and heat-flux measurements,[18] further supporting this numerical approach.

Even with no account of the reverse shock at the secondary diaphragm, the finite-rate simulations indicate a significant dissociated oxygen component for the air condition.

Table 2. Nominal 40 MJ/kg nitrogen freestream flow conditions, based on shot 163.

Property	Finite-rate CFD	Equil. CFD	Exp.	JUMP
Density, kg/m^3	1.846 x10^{-3}	1.612 x10^{-3}	-	1.718 x10^{-3}
Velocity, m/s	8439	8608	-	8284
Shock velocity, m/s	8233	8402	7808 - 8494	8284
Mach number	11	10.5	11.2	9.9
Static pressure, kPa	0.814	0.826	0.8 - 0.95	0.889
Static temperature, K	1444	1728	-	1555
Total enthalpy, MJ/kg	37.9	38.7	-	40.0
Pitot pressure, kPa	116.8	115	100 - 120	118
Unit Reynolds number, m^{-1}	304245	240221	-	257460
Ratio of specific heats	1.325	1.306	-	1.352
Specific gas constant, J/(kg-K)	305	297	-	333
N_2 mass fraction	0.9711	1.0	-	0.8780
N mass fraction	0.0289	0.0	-	0.1220

Table 3. Nominal 40 MJ/kg air freestream flow conditions, based on shot 169.

Property	Finite-rate CFD	Equil. CFD	Exp.	JUMP
Density, kg/m^3	2.826 x10^{-3}	1.410 x10^{-3}	-	1.836 x10^{-3}
Velocity, m/s	8230	8551	-	8284
Shock velocity, m/s	8059	8324	7868 - 8320	8284
Mach number	12.0	9.7	11.2	10.8
Static pressure, kPa	0.967	0.934	0.8 - 0.95	0.762
Static temperature, K	1036	2282	-	1168
Total enthalpy, MJ/kg	36.9	39.1	-	40.3
Pitot pressure, kPa	150	107	100 - 130	126
Unit Reynolds number, m^{-1}	549203	157660	-	325668
Ratio of specific heats	1.384	1.295	-	1.408
Specific gas constant, J/(kg-K)	330	290	-	355
N_2 mass fraction	0.7674	0.7483	-	0.7183
N mass fraction	0.0	0.0	-	0.0534
O_2 mass fraction	0.0450	0.2123	-	0.0011
O mass fraction	0.1608	0.0113	-	0.1982
NO mass fraction	0.0268	0.0145	-	0.0191

IV. Concluding Remarks

We can now obtain good estimates of all important flow properties in the test region of the X3 expansion tube. The interactions of the non-ideal driver, strong viscous effects in the acceleration tube, and finite-rate chemical kinetic effects have been reasonably well captured in the current numerical simulations.

The results are, however, not ideal and we need to do further work on a number of issues. These include the implementation of a multi-temperature thermochemical model, further increases in grid resolution, some type of non-ideal diaphragm model (especially for the light secondary diaphragm) and a more complete coupling between the models for the shock tube and acceleration tube. Also, the performance of the of the X3 free-piston compressor will be improved, possibly by building a new compression tube with larger diameter.

Appendix

The finite-rate chemistry model uses a specification file that is similar to Chemkin.[19] For the nitrogen test gas, we used the following species and reaction rates:[20]

```
SPECIES
   N2 N
END

REACTIONS         qss        cms  0.5
N2 + N2 <=> 2 N + N2               7.0e21      -1.6    1.132e5
                        REV/    1.09e16     -0.5    0.0/
N2 + N  <=> 2 N + N                3.0e22      -1.6    1.132e5
                        REV/        2.32e21     -1.5    0.0/
END
```

For air, we used the following species and reaction rate data:[21]

```
SPECIES
   N2 N O2 O NO He
END

REACTIONS  imp_euler  cms
N2 + N2 <=> 2 N + N2    1.92e17     -0.5    1.131e5
                    REV/ 1.09e16     -0.5    0.0 /
N2 + N  <=> 2 N + N     4.15e22     -1.5    1.131e5
                    REV/ 2.32e21     -1.5    0.0 /
N2 + O2 <=> 2 N + O2    1.92e17     -0.5    1.131e5
                    REV/ 1.09e16     -0.5    0.0 /
N2 + O <=> 2 N + O      1.92e17     -0.5    1.131e5
                    REV/ 1.09e16     -0.5    0.0 /
N2 + NO <=> 2 N + NO    1.92e17     -0.5    1.131e5
                    REV/ 1.09e16     -0.5    0.0 /
O2 + O  <=> 2 O + O     3.61e18     -1.0    5.94e4
                    REV/ 3.01e15     -0.5    0.0 /
O2 + N  <=> 2 O + N     3.61e18     -1.0    5.94e4
                    REV/ 3.01e15     -0.5    0.0 /
O2 + O2  <=> 2 O + O2   3.61e18     -1.0    5.94e4
                    REV/ 3.01e15     -0.5    0.0 /
O2 + N2  <=> 2 O + N2   3.61e18     -1.0    5.94e4
                    REV/ 3.01e15     -0.5    0.0 /
O2 + NO  <=> 2 O + NO   3.61e18     -1.0    5.94e4
                    REV/ 3.01e15     -0.5    0.0 /
NO + N2  <=> N + O + N2 3.97e20     -1.5    7.56e4
                    REV/ 1.01e20     -1.5    0.0 /
NO + N   <=> N + O + N  3.97e20     -1.5    7.56e4
                    REV/ 1.01e20     -1.5    0.0 /
NO + O2  <=> N + O + O2 3.97e20     -1.5    7.56e4
                    REV/ 1.01e20     -1.5    0.0 /
NO + O  <=>  N + O + O  3.97e20     -1.5    7.56e4
                    REV/ 1.01e20     -1.5    0.0 /
NO + NO  <=> N + O + NO 3.97e20     -1.5    7.56e4
                    REV/ 1.01e20     -1.5    0.0 /
NO + O  <=> O2 + N      3.18e9       1.0    1.97e4
```

```
                    REV/ 9.63e11      0.5    3.6e3 /
N2 + O  <=> NO + N      6.75e13       0.0    3.75e4
                    REV/ 1.5e13       0.0    0.0 /
END
```

Because the air test gas is more strongly influenced by the finite-rate chemistry in the unsteady expansion process, we look a little more critically at the validation of this model. Figure 6 shows the performance of the simulation code for air with finite-rate chemical reactions when modelling the flow over a half-inch sphere as studied by Lobb.[22] The shock detachment distance is quite sensitive to the modelling details. Although we are using a one-temperature thermochemical model, it performs reasonably well over a good range of the experimental data. As would be expected for a model which tends to overestimate the reaction rates, the CFD results head toward the equilibrium limit when they deviate from the experimental data.

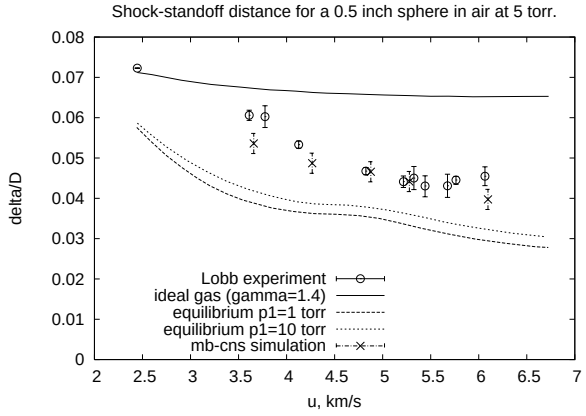

Figure 6. Normalised shock detachment distance for a 0.5 inch sphere travelling in air.[22] Only data points for an ambient pressure of 5 torr are shown.

Acknowledgments

The large calculations reported here were performed on a SUN Rack cluster computer sponsored by SUN Microsystems and the Queensland State Government.

References

[1]A. J. Neely and R. G. Morgan. The superorbital expansion tube concept, experiment and analysis. *The Aeronautical Journal*, 98(973):97–105, 1994.

[2]C. J. Doolan and R. G. Morgan. A two-stage free piston driver. *Shock Waves*, 9:239–248, 1999.

[3]B. S. Stewart, R. G. Morgan, and P. A. Jacobs. Rocketdyne hypersonic flow laboratory as high performance expansion tube for scramjet testing. *A.I.A.A. Journal of Propulsion and Power*, 19(1):98–103, 2003.

[4]T. J. McIntyre, I. Lourel, T. N. Eichmann, R. G. Morgan, P. A. Jacobs, and A. I. Bishop. An experimental expansion tube study of the flow over a toroidal ballute. *A.I.A.A. Journal of Spacecraft and Rockets*, accepted, 2003.

[5]A J Neely. *Planetary Entry Aerothermodynamic Studies in a Superorbital Expansion Tube*. PhD thesis, Department of Mechanical Engineering, The University of Queensland, Brisbane, Australia, 1995.

[6]R A Palmer. *Measurement of Heat Transfer in Superorbital Flows*. PhD thesis, Department of Mechanical Engineering, The University of Queensland, Brisbane, Australia, 1999.

[7]T. J. McIntyre, P. A. Jacobs, A. I. Bishop, and R. R. Boyce. Experimental and numerical studies of super-orbital ionising flows. In *22nd International Symposium on Shock Waves*, page Paper 1350, London, UK, July 1999. Imperial College.

[8]A J Neely and R G Morgan. The superorbital expansion tube concept, experiment and analysis. *Aeronautical Journal*, 98:97–105, March 1994.

[9]R G Morgan. *Handbook of Shock Waves, eds. G.Ben-Dor, O.Igra, T.Elperin*, volume 1, chapter Shock Tubes and Tunnels: Facilities, Instrumentation, and Techniques, Free-Piston Driven Expansion Tubes, pages 603–622. Academic Press, San Diego, 2001.

[10]H Mirels. Test time in low-pressure shock tubes. *The Physics of Fluids*, 6(9):1201–1214, September 1963.

[11]P. A. Jacobs. Shock tube modelling with L1d. Department of Mechanical Engineering Report 13/98, The University of Queensland, Brisbane, Australia., November 1998.

[12]P. A. Jacobs. Single-block Navier-Stokes integrator. ICASE Interim Report 18, 1991.

[13]P. A. Jacobs. MB_CNS: A computer program for the simulation of transient compressible flows. Department of Mechanical Engineering Report 10/96, The University of Queensland, Brisbane, December 1996.

[14]B. J. McBride and S. Gordon. Computer program for calculation of complex chemical equilibrium compositions and applications II. Users manual and program description. Reference Publication 1311, NASA, June 1996.

[15]R. J. Gollan. Yet another finite-rate chemistry module for compressible flow codes. Department of Mechanical Engineering Report 2003/09, The University of Queensland, Brisbane, July 2003.

[16]R J Bakos and R G Morgan. Chemical recombination in an expansion tube. *AIAA Journal*, 32(6):1316–1319, June 1994.

[17]G. J. Wilson, M. A. Sussman, and R. J. Bakos. Numerical simulations of the flow in the HYPULSE expansion tube. Technical Memorandum 110357, NASA, June 1995.

[18]T. B. Silvester. Experimental and numerical investigation of multidimensional hypervelocity flows. PhD thesis, The University of Queensland, Brisbane, Australia., March 2005.

[19]R. J. Kee, F. M. Rupley, and J. A. Miller. CHEMKIN-II: A FORTRAN chemical kinetics package for the analysis of gas-phase chemical kinetics. Report SAND89-8009, Sandia National Laboratories, Livermore, CA 94551, September 1989.

[20]C. Park. *Nonequilibrium hypersonic aerothermodynamics*. John Wiley and Sons, New York, 1990.

[21]R. N. Gupta, J. M. Yos, R. A. Thompson, and K. P. Lee. A review of reaction rates and thermodynamic and transport properties for an 11-species air model for chemical and thermal nonequilibrium calculations to 30000 K. NASA Reference Publication 1232, 1990.

[22]R. K. Lobb. Experimental measurement of shock detachment distance on spheres fired in air at hypervelocities. In W. C. Nelson, editor, *The High Temperature Aspects of Hypersonic Flow*, pages 519–527, Oxford, 1964. Pergamon Press.